CHARACTERIZATION OF PORPHYRIN THIOL ASSEMBLIES ON AU (111)

A Senior Scholars Thesis

by

KATHRYN M. WEBB

Submitted to the Office of Undergraduate Research
Texas A&M University
in partial fulfillment of the requirements for the designation as

UNDERGRADUATE RESEARCH SCHOLAR

April 2009

Major: Chemistry

CHARACTERIZATION OF PORPHYRIN THIOL ASSEMBLIES ON AU (111)

A Senior Scholars Thesis

by

KATHRYN M. WEBB

Submitted to the Office of Undergraduate Research
Texas A&M University
in partial fulfillment of the requirements for the designation as

UNDERGRADUATE RESEARCH SCHOLAR

Approved by:

Research Advisor: James D. Batteas
Associate Dean for Undergraduate Research: Robert C. Webb

April 2009

Major: Chemistry

ABSTRACT

Characterization of Porphyrin Thiol Assemblies on Au (111). (April 2009)

Kathryn M. Webb
Department of Chemistry
Texas A&M University

Research Advisor: Dr. James D. Batteas
Department of Chemistry

Numerous studies have been conducted using porphyrin molecules on various substrates to investigate their diverse photoelectrochemical, catalytic, electronic, and biochemical properties. These properties make porphyrin molecules targets for use as active components in devices such as chemical sensors, information storage, and photo sensitizers in solar cells. In this study, we investigated the assembly and aggregation of mono-podal zinc (II) porphyrin molecules into a dodecanethiol self-assembled monolayer (SAM) on gold. The porphyrin macrocycle is attached to a phenyl linking group and an alkanethiol tether which binds to the gold surface. The charge transport properties of the porphyrin in confined geometries are being investigated based on previous studies of aggregated assemblies on gold surfaces. In these studies, we find small islands of porphyrins to produce unique electrical switching behavior not observed in single molecules. To explore how island size influences the electrical properties of these compounds, we are investigating ways of creating well defined directed assemblies of controlled nanoscale dimension ranging from 10 to 100 nm in size by Atomic Force

Microscopy. This research will facilitate the development of nanoscale and molecularly enhanced devices for applications such as light harvesting or sensing.

DEDICATION

For my family, who always encourage and support me in my decisions. For my teachers, Mrs. Janie Mueller and Dr. John Hogg, who ignited my desire to pursue my degree in chemistry. Without them, I would not be here.

ACKNOWLEDGMENTS

Many hours have been devoted to this research project, and there are many people who deserve to be acknowledged for their extensive effort and dedication. I wish to acknowledge and thank my research advisor and mentor, Dr. James Batteas, for accepting me into his research group as an undergraduate to further my experience in academic research and materials science. I also wish to thank Amanda Schuckman who has graciously accepted me to contribute work on her project. She has spent countless late nights working with me on the instrument, answering my numerous questions, and providing useful discussions. Ryan Jones has also been a tremendous help with my inquiries and troubleshooting problems on the Atomic Force Microscope. With that, I would like to acknowledge the Batteas Research Group at Texas A&M University. They have all been a source of encouragement and support throughout my undergraduate research experience.

Thank you to my close friend and fellow chemistry major, Jamie Wheeler, for all our late nights studying and working in the lab. I am inspired by your support and dedication and thank you so much for all your encouragement. She is the one who encouraged me to apply for the Undergraduate Research Scholars Program and I am forever thankful for her pushing me to my fullest potential.

I would like to acknowledge the Texas A&M Chemistry Department for the Emile Schwiekert Endowed Scholarship in Chemistry for the 2008-2009 school year. Without the support of the Chemistry Department, I could not financially attend this university and experience this program and the people I have encountered.

The Undergraduate Research Scholars Program has been an amazing opportunity to undergo a research project for a year and present and complete a thesis on the work. The office has been extremely helpful with advice for better writing and researching techniques. Thank you for your support and encouragement throughout the program duration.

Lastly, I want to acknowledge the grants that support this research: Texas A&M University, THECB – Norman Hackerman Advanced Research Program (Grant 010366-0006-2006), and the TAMU Energy Resources Program. We also acknowledge Professor Mike Drain of Hunter College /CUNY for supplying the porphyrin compounds.

NOMENCLATURE

AFM	Atomic Force Microscopy
FT-IR	Fourier Transform Infrared Spectroscopy
SAM	Self-Assembled Monolayer
STM	Scanning Tunneling Microscopy

TABLE OF CONTENTS

LIST OF FIGURES

CHAPTER I

INTRODUCTION

Atomic Force Microscopy (AFM) has been traditionally used to visualize surface topography such as roughness, defects and physical height differences of molecules.[1] Constructively, the technique of nanografting has provided a functional complement to the use of AFM by having the ability to determine the molecular physical height on various substrates by utilizing an internal reference.[1] Self-assembled monolayers (SAMs) have been increasingly utilized as internal references for nanografted molecules due to their stable, well-ordered, and densely packed structures that can be formed on metal surfaces through sturdy thiol linker (S-Au) chemical bonds.[2,3] Due to the thiol linker as the attachment to the electrode, alkanethiol SAMs have been the primary internal reference implemented in nanografting for use in molecular electronics because they have been extensively studied by AFM and have distinguished structures and properties.[4] Figure 1 displays an image of an *n*-dodecanthiol SAM and shows the orientation of the molecules on the surface of the gold.

This thesis follows the style of *Journal of Physical Chemistry C*.

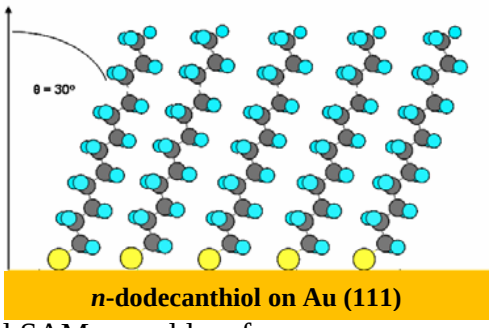

Figure 1. *n*-dodecanethiol SAM on gold surface.

Thus, the height difference of the grafted molecules can then be accurately quantified by direct comparison to the reference alkanethiol molecules.[5]

In recent developments, thiol-terminated molecules on gold surfaces have been extensively researched for the advancement and understanding of the charge transport properties that affect future molecular electronics.[6-9] Specifically, porphyrin molecules have been studied expansively due to the variety of their chemical and electrical properties: photoelectrochemical,[10] electronic,[11] and bioanalytical.[12,13] The combination of their diverse characteristics facilitates their application as active components in molecular devices for use in chemical sensors,[14,15] memory storage,[16] and solar cells.[17] One advantage in the numerous electronic device applications is the propinquity of the HOMO state of the porphyrin molecule to the Fermi level of the gold surface to which it is bonded.[18] The greater part of these research studies and applications have focused on single molecules and monolayers on the different surface substrates. However, in any future molecular electronics device, junctions containing of porphyrin thiol-terminated molecules on the order of 10's to 1000's are more likely to be implemented due to large

scale production and fabrication. Domain size and molecular conformation of how the molecules fit into the aggregate may affect the important properties of porphyrins.

One related study to the affect of domain size on the charge transport property has been conducted where a self-assembled mixed monolayer of *n*-dodecanethiol and the free base derivative of the molecule of interest, 5,10,15-tri(4-pyridyl)-20-perfluorophenylporphyrin thiol was prepared.[18] The free-base porphyrin thiols self-assembled into aggregates of 2 nm and 6 nm areas within the SAM. Using Scanning Tunneling Microscopy (STM), these aggregates have demonstrated uncontrollable stochastic switching due to the random conformations of the molecules,[18] where the molecules randomly turned "on" and "off," in terms of their conductance. These unique properties of porphyrins need to be controlled in future nanoscale applications in order to be beneficially applied.

The addition of a zinc (II) metal to the center of the porphyrin macrocycle, Zn (II)-5,10,15-tri(4-pyridyl)-20-perfluorophenylporphyrin thiol (Zn (II) porphyrin thiol), has allowed for controllable bias-induced switching. Under visualization with the STM, the aggregate apparent height has increased with applied bias from 1.4 V to 2.0 V. Figure 2 displays the increase in aggregate apparent height with the application of a higher voltage. The bright spots indicate that the molecules have "turned on" to a higher conductance state with an increase in bias.

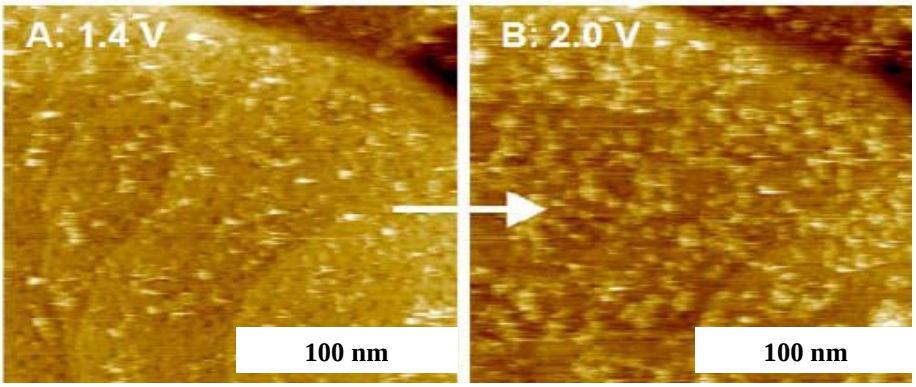

Figure 2. STM images of zinc (II) porphyrin thiol aggregates by indirect self assembly A. Bias of 1.4 V B. Bias of 2.0 V

The Zn (II) porphyrin thiol (Figure 3) self-assembled into aggregates in the range of 3-25 nm wide. The proposed optimal size for the controlled bias-induced switching is 10 nm. Aggregates smaller than 10 nm in width would have too few molecules to exhibit the electrical property while aggregates larger than 10 nm in width would not be practical in future nanoscale applications due to the sheer number of molecules contained in the large area.

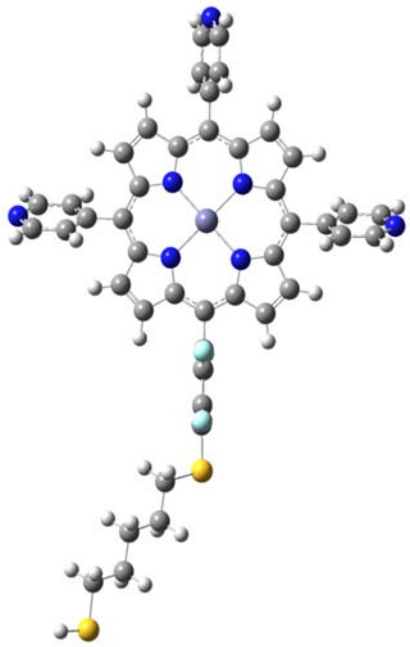

Figure 3. Structure of 5,10,15-tri(4-pyridyl)-20-biperfluorophenylporphyrin thiol. The Zn (II) addition is in the middle of the porphyrin ring.

The focus of this thesis lays on the direct assembly of metallic porphyrin thiol aggregates with one thiol surface linking group in confined geometries on gold substrates to determine size domain effects on switching properties for future application in nanoscale electronics. The metallic mono-podal Zn (II) porphyrin thiol molecules have been nanografted into SAMs of *n*-dodecanethiol which functioned as an internal reference for the new molecules to compare their structure and electrical properties. To create the nanoscale spatially confined structures of the Zn (II) porphyrin thiol aggregates, the *n*-dodecanethiol reference monolayer was shaved away from the gold surface in a predetermined area, Figure 4, using force to displace the dodecanethiol layer but not remove the gold surface atoms.

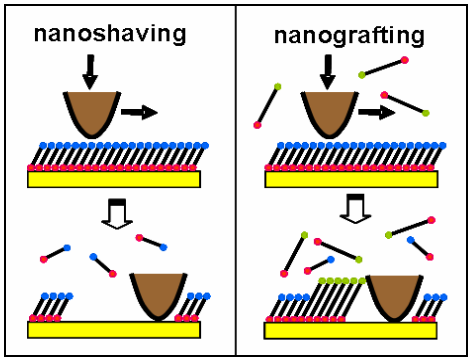

Figure 4. Illustrations of nanoshaving and nanografting. During nanoshaving, only the surface monolayer was displaced from the gold and a nanowell was made displaying an empty hole. During nanografting, the surface monolayer was displaced from the gold; however, new molecules attach to the gold surface as soon as the monolayer was displaced. A comparison can then be made between the height differences of the new molecule and the alkanethiol monolayer.

Nanoshaving creates a square hole on the flat surface that can be seen with the AFM tip by use of a topography scan.[1] The squares ranged in size from 100 nm to 10 nm, with 10 nm being the ultimate goal for the optimization and observation of the desired electronic properties. Figure 5 shows a series of patterned nanowells in an *n*-dodecanehthiol SAM matrix.

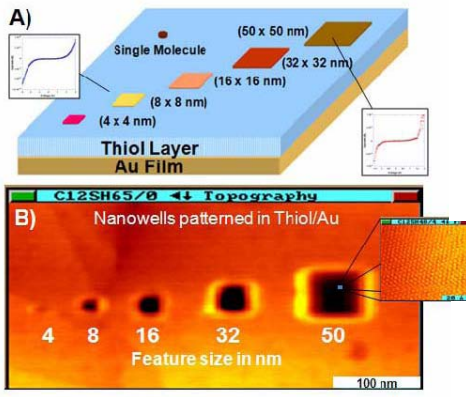

Figure 5. AFM topography scans of nanoshaving and nanografting. A. Illustration of various nanowells that can be made in the alkanethiol monolayer. B. Topography scan of various sized nanowells after nanoshaving the alkanethiol monlayer.

After assembly, the patterned area was re-imaged to examine the structure and physical height of the patterned assemblies. The reference molecule, *n*-dodecanethiol, stands at approximately 12 Å thick on the surface of the gold at an angle 30˚ from the surface normal. The physical height of this monolayer was compared to that of the assembled porphyrins to deduce their molecular height on the surface.

The thiol linker group was thought to increase the propensity for surface bonding to the Au (111) surface for nanografting. Also, the addition of Zn (II) metal to the porphyrin macrocycle was known to increase its affinity for aggregation due to the high π-π coupling energy of the pi electrons and may help drive the ability to graft the molecule onto the surface of the gold.[19] Once grafted, the charge transport properties of the Zn (II) porphyrin aggregates in the 10 nm confined spaces will be analyzed using STM to observe how directed assembly dimension influences conduction properties.

Understanding how the zinc (II) porphyrin molecules have assembled in the confined aggregates and how the domain size of the aggregates influences the conduction and charge transport properties due to neighboring interactions by pi stacking is essential. In addition, the direct assembly control of molecules that create electrical junctions in confined geometries has been vital to the progress and execution of modern and future molecular nanoelectronic devices whose function is based heavily on charge transport properties. The general goal of this research was to investigate the parameters necessary to achieve a high density of molecular ensembles of 10 nm in width of the Zn (II)

porphyrin thiol by directed assembly in an effort analyze the domain charge transport properties by STM in order to advance the nanoelectronic industry with future applications in solar cells and electronic devices.

CHAPTER II

METHODS

Materials

The SAMs were prepared on flame annealed ~150 nm Au (111) films on mica received from Molecular Imaging-Agilent from Phoenix, Arizona. Dodecanethiol (DDT) was purchased at 98% purity from Aldrich and used as received.

Preparation of self-assembled monolayers

UV/ozone was applied to the flame annealed Au (111) substrates purchased from Molecular Imaging, Inc. for 20 minutes in order to remove impurities and contamination from the surface of the gold film. Following the UV/ozone treatment, the gold film was rinsed with high purity (18.2 MΩ•cm) water (NANOpure Diamond, Barnstead) and ethanol. Finally the gold film was dried with streaming nitrogen gas. The *n*-dodecanethiol SAM was created by soaking the Au (111) substrate in 1mM *n*-dodecanethiol in ethanol for 24 -72 hours. After 24-72 hours of immersion in the 1mM solution has passed, the Au (111) substrate was rinsed liberally with ethanol and was dried with streaming nitrogen.

Atomic force microscopy

The AFM used in the experiments was a Molecular Imaging 4500 Pico SPM (Agilent, Phoenix, AR) with a deflection-type detection scanning head interfaced with an

SPM1000 control electronics Revision 8 (RHK Technology Inc., Troy, MI). All AFM images were collected in contact mode under dichloromethane in a home built Teflon cell. The AFM tips used were commercially available Si_3N_4 AFM tips (Veeco/TM Microscopes in Sunnyvale, CA.) with a nominal tip radii of 10 nm and a nominal spring constant of 0.5 N/m.

Zinc (II) porphyrin thiol

The Teflon sample cell for the AFM and the crystal sample tip holder were cleaned in ethanol and dichloromethane by sonicating in each solvent for one hour prior to the experiment. The contents were then rinsed with ethanol and were dried with streaming nitrogen gas. The AFM tip and laser were set up and optimized for maximum laser signal (~275 a.u.) in order to image friction and topography scans of the SAM. For grafting the Zn (II) porphyrin thiol with the AFM tip, the SAM was placed in the sample cell under dichloromethane. The AFM tip scans the surface of the SAM collecting images of topography and friction data. A smooth gold terrace was selected from the image and a variable bias voltage was added to the tip to push it down into the *n*-dodecanethiol molecules while it scanned, shaving away the molecules. This technique is known as nanoshaving. Nanoshaving was done with the sample in dichloromethane with no added molecules in order to find the optimal bias voltage to successfully remove all of the *n*-dodecanethiol molecules from the surface of the gold creating a confined nanowell (see Figure 6).

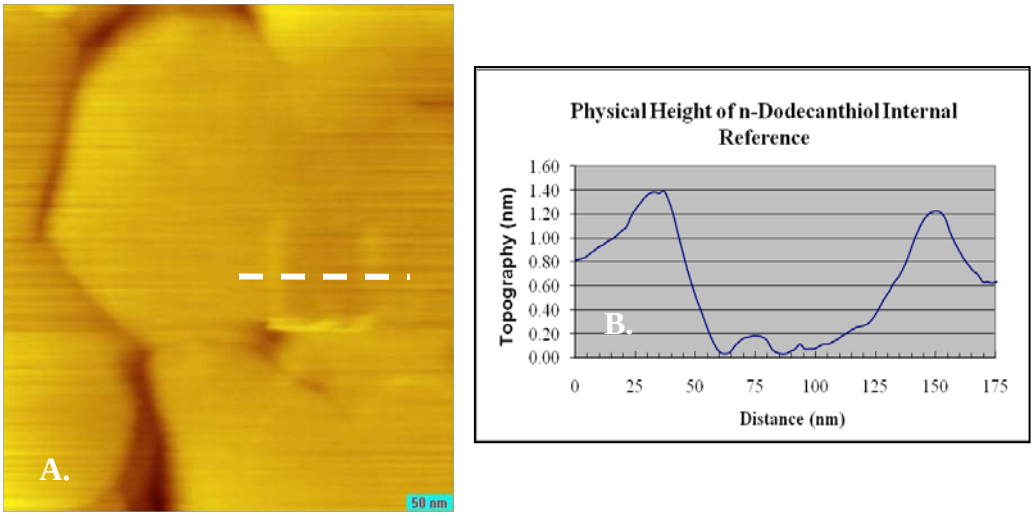

Figure 6. Topography image of a confined nanowell. A. Topography image of a confined 100 nm nanowell in internal *n*-dodecanethiol reference matrix. B. Physical height of internal reference is ~12Å.

Next the 64 μM Zn (II) porphyrin thiol was added slowly to the sample cell. This was done carefully with syringes and tiny tubing to minimize the disturbance of the AFM tip placement. After the porphyrin solution has been inserted into the sample cell, the same procedure was followed as stated above. A bias voltage was applied to the tip and as the *n*-dodecanethiol molecules were shaved away from the surface of the gold, the Zn (II) porphyrin molecules were inserted into the nanowell following the progression of the AFM tip. This technique is known as nanografting and is a type of directed assembly of molecular aggregates into a SAM. Once the square has been made, a new image was scanned of the surface without applying a bias to determine if the Zn (II) porphyrin molecules have been within the confines of the square onto the surface of the gold. The height difference between the *n*-dodecanethiol molecules and the Zn (II) porphyrin molecules was determined from the topography scans. Parameters such as the grafted

area, the scan speed, and the number of scans at which the tip shaves the *n*-dodecanethiol molecules have been optimized for the 10 nm squares.

CHAPTER III

RESULTS

FT-IR measurements

A proposed model of the Zn (II) porphyrin thiol embedded in an *n*-dodecanthiol SAM tilting away from the surface normal by 42˚ is illustrated in Figure 7, where α is 42˚ and θ is 48˚. The in-plane pyrrole ring breathing mode, a_1, and out-of-plane pyrrole C-H bending mode, a_2, are shown in the figure. The tilt angle of the Zn (II) porphyrin macrocycle (α) with respect to the gold surface normal has been derived from the intensity ratio of the two modes in the IR spectrum using a previously published method.[20]

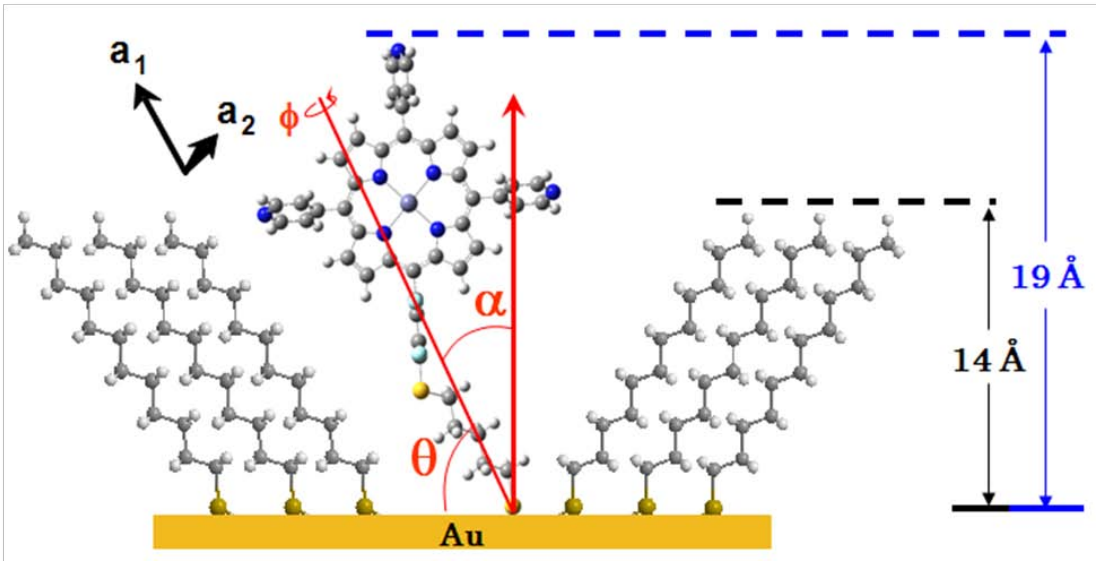

Figure 7. Proposed binding scheme of zinc (II) porphyrin in an *n*-dodecanethiol SAM.

From the tilt angle calculated from FT-IR measurements, the height of the Zn (II) porphyrin thiol was calculated to be 19 Å. Therefore, the height difference between the reference SAM monolayer and the grafted metalloporphyrin molecule is ~5 Å. This height difference of the monolayer has been confirmed by AFM imaging.

Calculation of Zn (II) porphyrin thiol by Beer's Law

The Zn (II) porphyrin thiol has been dissolved in 10 mL dichloromethane. The concentration was unknown and UV-Vis absorption spectroscopy has been performed to calculate the unknown concentration based on a known concentration of stock solution. The stock solution is 0.5 mM Zn (II) porphyrin thiol and was diluted to make four calibration standards. The four calibration standards concentrations were 7.6, 4.1, 2.2, and 1.5 μM, respectively. Each solution was placed in a clean quartz cuvette in a UV-Vis spectrometer encased in a black box. The absorption of the UV-Vis light was measured for each solution in order to obtain a linear regression calibration plot. Figure 8 displays the calibration graph of the Zn (II) porphyrin thiol calibration standards. Beer's Law states that the absorbance of a solution is directly proportional to the concentration. A plot of absorbance versus concentration yields a straight line due to their linear relationship. The equation for the linear regression line can be used to determine the concentration of an unknown solution once the absorbance has been measured.

$$A = \varepsilon bc$$

Where A is the absorbance, ε is the molar absorptivity coefficient of the Zn (II) porphyrin thiol, b is the pathlength of the quartz cuvette in centimeters, and c is the concentration of the solution. From the linear regression calibration graph, the molar absorptivity coefficient is the slope of the calibration line and is 100.27 mM^{-1} cm^{-1}.

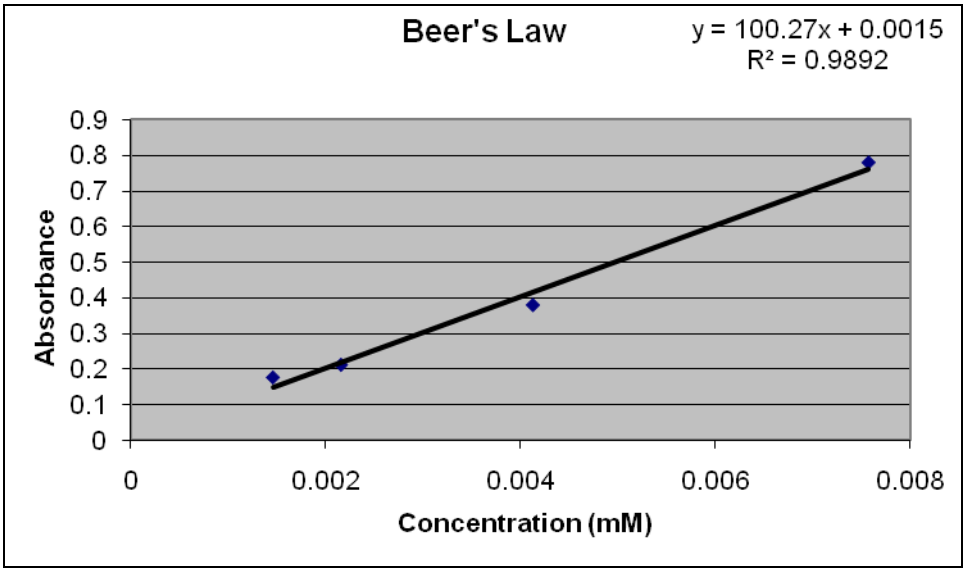

Figure 8. Linear regression calibration graph of Zn (II) porphyrin thiol

From the linear regression obtained in the calibration graph from the standards made from the stock solution, the unknown original concentration of the Zn (II) porphyrin thiol was calculated to be 64 μM. The following AFM nanografting experiments have been used with the Zn (II) porphyrin thiol concentration of 64 μM.

Calculation of imaging and nanografting forces with AFM tip

The AFM feedback loop relies on the forces generated between the AFM tip and the sample. The imaging and nanografting forces were calculated based on measuring the deflection of the lever, and knowing the stiffness of the cantilever. In a force-distance

curve, the cantilever is guided by a piezoelectric actuator to push against the gold film surface until the tip bends.[21] The force applied to the sample surface is called the jump to contact force. The AFM tip traces over the sample for a specified distance. The force-distance curve is obtained by measuring the AFM tip-sample interaction force along the cantilever during the jump to contact and retraction process. The slope of the line on the force-distance curve is calculated from the pull off force associated with the retraction of the tip off the sample surface. The force applied over the distance imaged is in MV/nm. The AFM tip has a manufacturer reported spring constant of 0.5 N/m. For the AFM tips used (Veeco), there were two force distance curves obtained with an average slope of 115 MV/m, or 0.115 V/nm on the nanoscale level. The imaging force of the tip on the surface of the sample was calculated to be over the range of ca. 5-8 nN based on a jump to contact force of 1.2-1.8 volts. In nanografting molecules on the sample surface, the jump to contact force of the tip to the sample and the bias applied to the tip to shave the internal reference molecules were additive. The bias applied during nanografting is 3.5 volts and the jump to contact bias was in the range of 1.2-1.8 Volts. Thus the range of nanografting forces for the AFM tip for the force-distance slope of 115 MV/m is ca. 20-23 nN.

Surface imaging

AFM has been employed in order to examine the surface structure of the inserted Zn (II) porphyrin molecules into the *n*-dodecanethiol monolayer on the surface of the Au (111). AFM images after nanografting display squares inserted into the monolayer matrix,

suggesting that the Zn (II) porphyrin molecules are sticking up out of the background matrix. As determined by contact mode images in dichloromethane, the physical heights of the Zn (II) porphyrin thiols were observed to extend above the *n*-dodecanethiol monolayer matrix SAM anywhere from 3-30 Å. The variation of height difference was likely due to differences in bonding location, such as near defects in the film. The height variation can also be attributed to the size of the confined nanowell created, and the amount of scans the tip has passed over the gold surface. The basic trend observed was the smaller the confined island of molecules, the smaller the height difference between the reference matrix and the Zn (II) porphyrin thiol. The Zn (II) porphyrin thiol monolayer should have a height difference of about ~5 Å from the *n*-dodecanthiol SAM. The larger the confined squares, the longer the AFM tip was scanning over the gold surface, and the higher the physical height of the inserted molecules due to the possibility of the formation of bilayers or stacking of the Zn (II) porphyrin thiol .

Manually shaved square

The Zn (II) porphyrin thiol molecule has been attempted to be grafted into manual shaved/grafted square geometries of ranging from 10 to 100 nm in size with the AFM tip. Due to the large size of the AFM tip radius (ca. 10 nm), sufficiently high resolution images were nearly impossible to achieve in order to detail the molecular organization of the *n*-dodecanethiol matrix.

The smallest island obtained by manual optimization of AFM parameters was 50 nm. This is due to the rapid evaporation of the solvent dichloromethane. However, at this time there has not been a solution to prevent the evaporation of the solvent. The Zn (II) porphyrin is only soluble in one other solvent, chloroform, but for health and safety reasons it has not been tried as a potential solvent for AFM imaging. Due to the rapid evaporation of dichloromethane, it was difficult for the AFM tip to stabilize on the surface of the SAM for a long enough time period to nanograft and image the resulting molecular islands. Figure 9 displays a 50 nm and a 100 nm confined island.

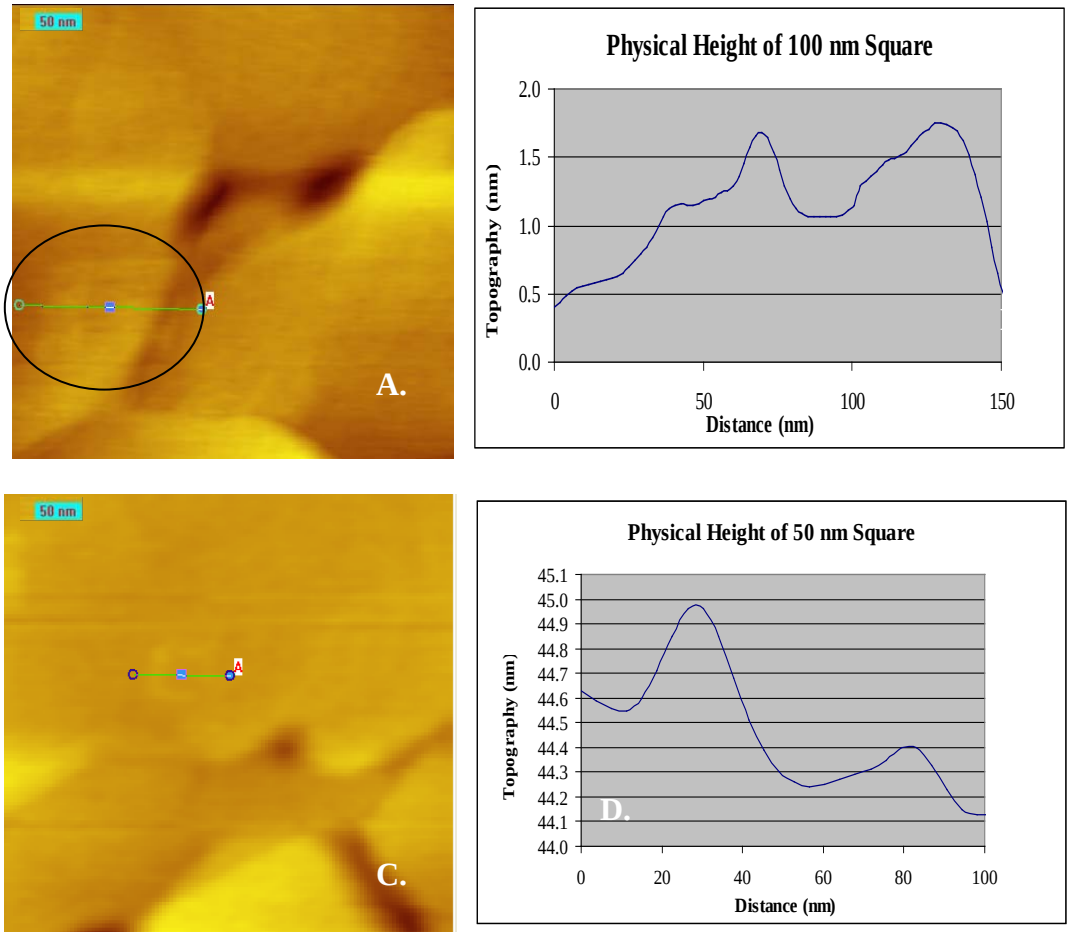

Figure 9. 100 nm and 50 nm grafted square topography scans. A. Topography image of a 100 nm square of nanografted Zn (II) porphyrin. The physical height is 25 Å. B. Line trace of the physical height of 100 nm square. C. Topography image of a 50 nm square where only the edges grafted the Zn (II) porphyrin. D. Line trace of the physical height of 50 nm square.

Scan speed, scan number and bias voltage were adjusted in order to optimize nanoshaving of the background matrix. The optimal parameters were 20 ms scan speed, 5 scans over the area, and a bias of 3.5 V. In order for the Zn (II) porphyrin thiol to have a clean gold surface to attach, all of the matrix molecules must be removed during the nanografting process.

Manual squares have also been attempted for smaller squares from 10-50 nm in size. In order to be able to see if the 10 nm squares are successfully grafted, a large pattern must be made due to the minute size of each square. However, large patterns of 10 nm square size were not possible to obtain by manual manipulation of the AFM tip due to poor resolution and rapid solvent evaporation that disturbed the AFM tip and diminished the feedback signal.

Lithography

Lithography is a technique used to engrave patterns on a surface using a computer software program to control the movement and force applied to the AFM tip. Lithography programs have been used to investigate observations based on the binding patterns of the Zn (II) porphyrin thiols and whether different shapes and parameters will nanograft the porphyrin molecules more successfully than others.

Several different lithography patterns have been implemented. One lithography pattern has been programmed to nanograft the Zn (II) porphyrin thiol molecules into a 4x4 array of circles (Figure 10). These circles were arranged in a four leaf clover shape, and the AFM tip scanned each circle 5 times. The width of each circle was ~10-20 nm, which is the optimal size of the confined domain desired. From the topography images achieved, the Zn (II) porphyrin thiol readily grafted into this pattern of circles. The physical height of the outer circles was ~3-5 Å, which is consistent with the calculated monolayer height. Figure 11 displays a topography image of this script. Since the AFM tip has

scanned the middle of the array of circles more than the outer edges of the circles, the physical height in the middle of the circles (14 Å) was higher than the height observed on the cross section of a single circle. The successful nanografting of the Zn (II) porphyrin molecules was reproducible using this lithography script.

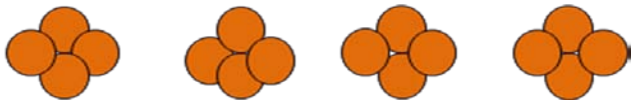

Figure 10. Schematic of circle pattern lithography script, 1x4 section of the 4x4 array.

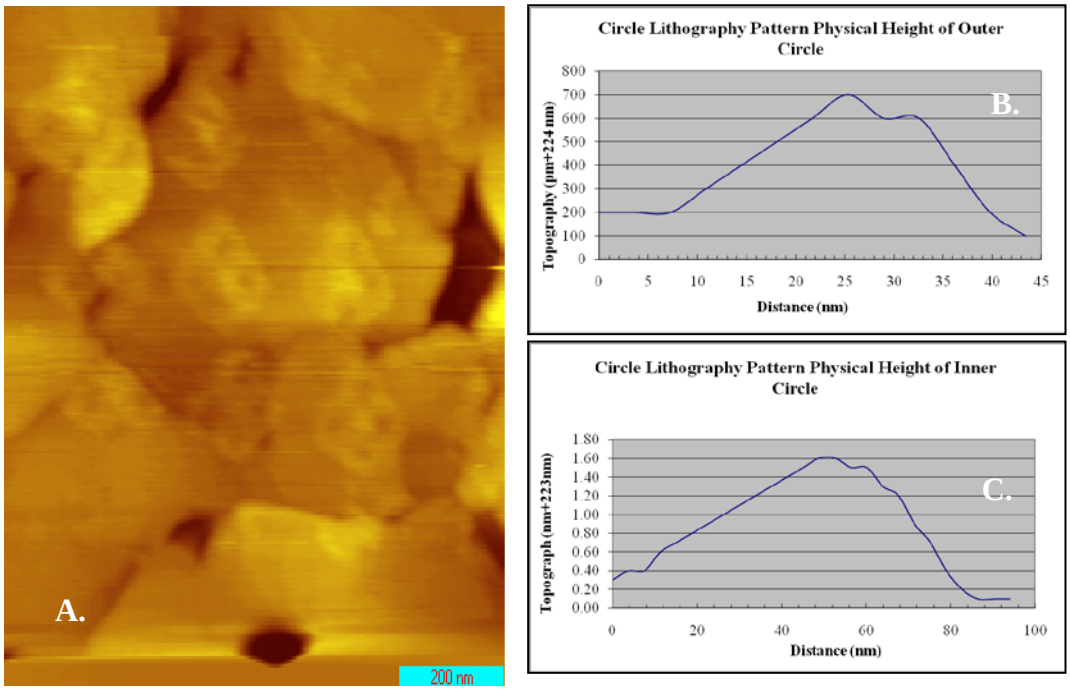

Figure 11. Topography and physical height of circle lithography script. A. Topography image after lithography. B. Physical height of one outer ring. C. Physical height of one center of circle structure.

A second lithography pattern implemented to nanograft the Zn (II) porphyrin thiol molecules was an 8x8 array of 50 nm frames spaced 70 nm apart (Figure 12). The

pattern was successful in nanografting the Zn (II) porphyrin consistently. The physical height of the Zn (II) porphyrin thiol was observed to be between 10-20 Å. This physical height was not consistent with the calculated height of the monolayer of the Zn (II) porphyrin thiol. The increase in physical height compared to the background matrix was due to the 50 nm frame size. The increase in physical height was proportional to the size of the surface area nanografted by the AFM tip. The proposed mechanism is that the AFM tip scans over the surface area more times with a larger surface area causing the porphyrin molecules to stack on top of each other causing the increase of physical height seen in the topography image. Figure 13 displays a 50 nm frame topography image after lithography.

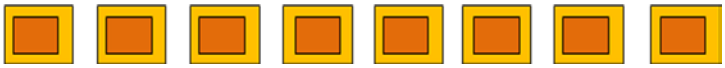

Figure 12. Schematic of the 50 nm frames lithography script, 1x8 section of the 8x8 array.

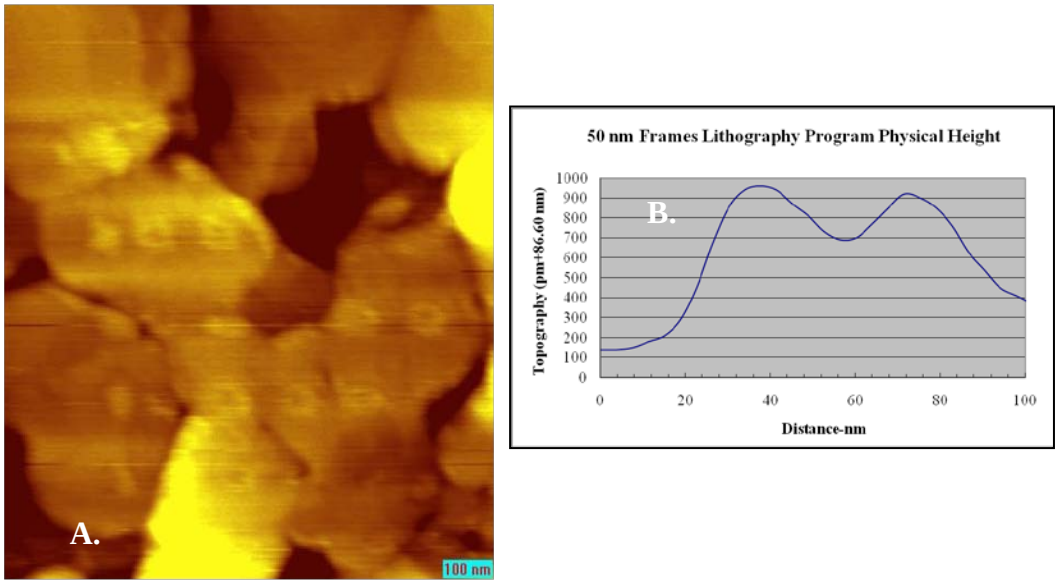

Figure 13. Topography and physical height of 50 nm frames lithography script. A.Topography image after lithography of an 8x8 array of 50 nm frames. B. Physical height of one 50 nm frame.

The lithography program for the 50 nm patterned array of frames has been modified to graft the Zn (II) porphyrin thiol into 10 nm patterned frame arrays. The script was fast, takes less than one minute, and the solvent has remained stable enough to retrieve topography images of the patterned array due to the rapid nature of the program. The 10 nm patterned squares were grafted successfully and seen in the topography images as bright dots. Due to the sharp radius of curvature of the tip, the observed porphyrin islands were ~20 nm in width and did not resemble a frame, but a filled in square. Patterning arrays of 10 nm frames might be better than patterning arrays of squares due to the fact that the tip does not spend a lot of time in the center of the square. Thus, this technique has grafted monolayers rather than bilayers or stacks of the Zn (II) porphyrin thiol. The physical height of the 10 nm frame was observed to be ~3-6 Å, consistent

with the calculated physical height of the porphyrin monolayer. Figure 14 displays the topography images of the 10 nm patterned array, which was reproducible.

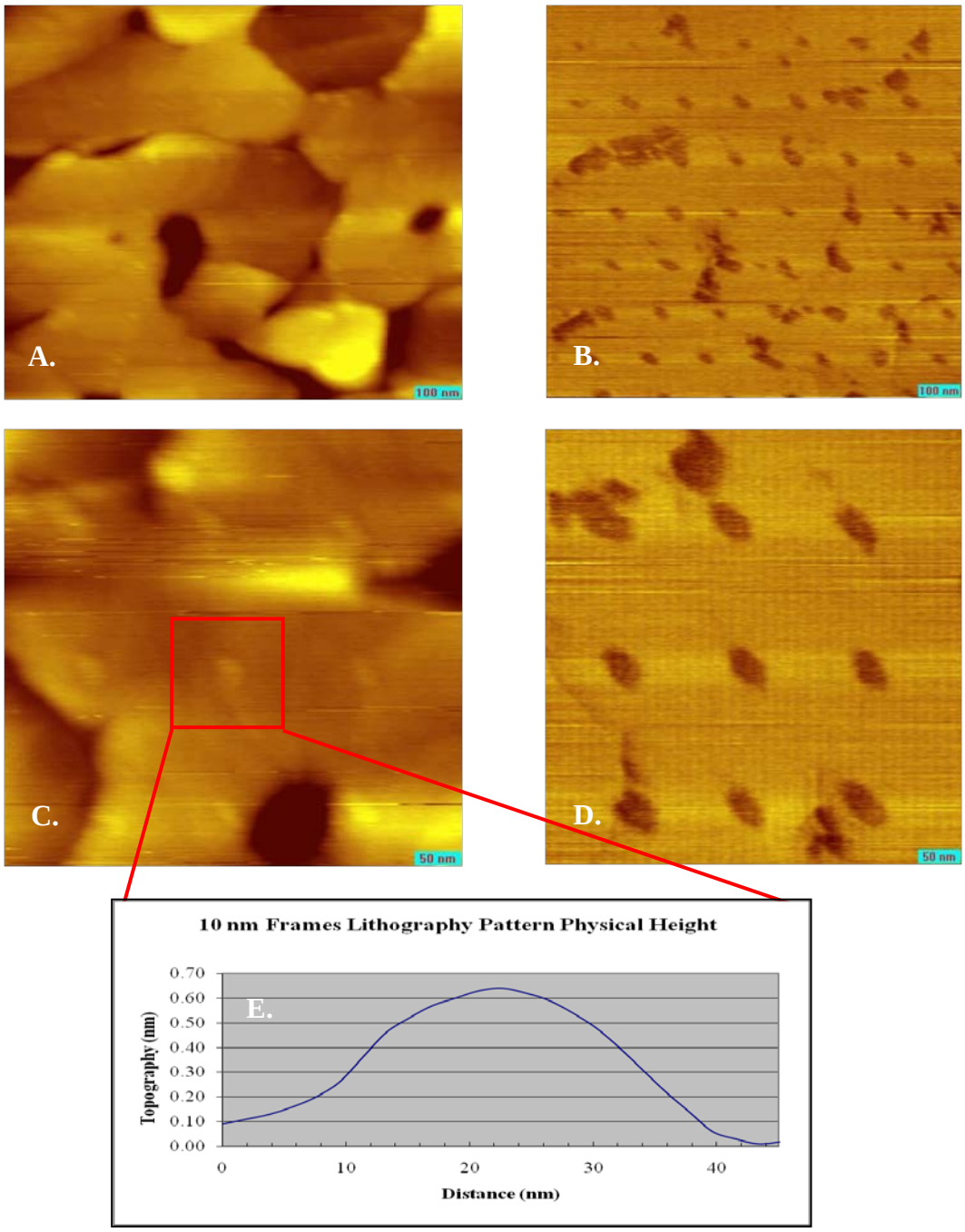

Figure 14. Topography image of an 8x8 array of 10 nm Zn (II) porphyrin frames. A. Topography image of lithography at 1 µm. B. Friction image of array at 1 µm. C. Topography image of lithography at 500 nm. D. Friction image of array at 500 nm. E. Physical height of squares is 6 Å.

Future steps

The Zn (II) porphyrin thiol was successfully grafted into an 8x8 array of 10 nm squares. Next steps are to pattern a large area of these 10 nm squares, 3μm x 3μm, in order to move the gold sample to the STM and easily locate the nanografted patterned area. The proposed method of transfer is displayed in Figure 15. The Au (111) sample will be divided into 3 μm alternated strips of gold and mica in order to confine the gold area available for nanografting. The nanografted pattern of squares will be located easier in the STM due to the smaller surface area of the gold. This can be done using a PDMS stamp and gold etching in order to remove the unwanted gold from the mica substrate. A tiny scratch will be made at the top of the gold sample and then the nanografted squares will follow along the strip of gold. After the nanografted squares are complete, the AFM tip will be used to make a scratch in the surface of the gold following the pattern of squares.

The two scratches allow for upper and lower boundaries for easier location of the patterned Zn (II) porphyrin thiol squares in the STM.

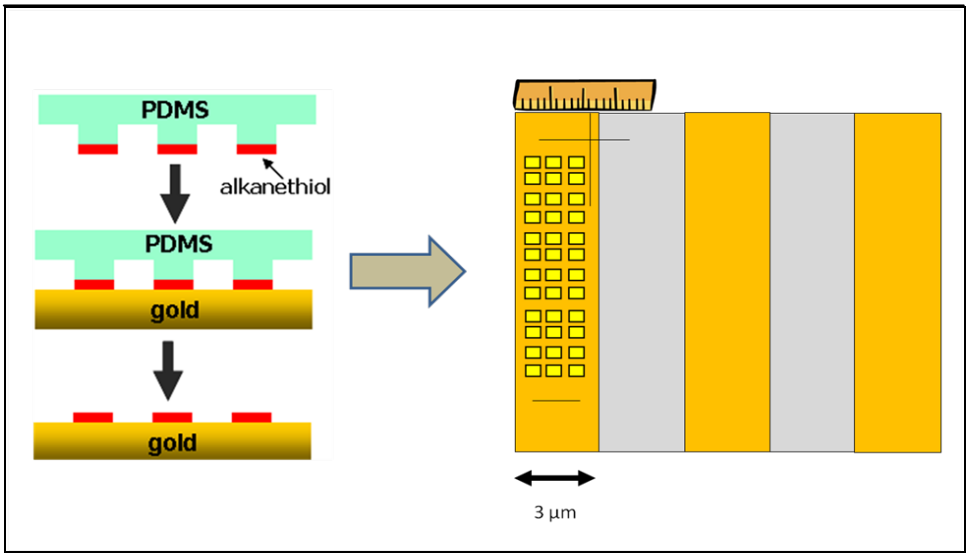

Figure 15. Future method for transfer from the AFM to STM.

In the STM, the charge transport properties of the Zn (II) porphyrin islands will be analyzed to determine the optimal cluster size for the bias-induced switching behavior from the directed assembly of the molecules.

CHAPTER IV

SUMMARY AND CONCLUSIONS

Various studies have been conducted using porphyrin molecules on various substrate surfaces because the molecules exhibit assorted photoelectrochemical, electronic, and bioanalytical properties that enable their widespread application in nanotechnological devices such as chemical sensors, memory storage, photo sensitizers, and organic solar cells. In this study, we have investigated how specific zinc (II) porphyrin thiol molecules attached to a thiol tether assemble and aggregate into predetermined confined islands into an *n*-dodecanethiol self-assembled monolayer. The nanografting technique utilizing Atomic Force Microscopy has spatially organized the Zn (II) porphyrin thiol molecules into previously determined 10 nm confined assemblies. Lithography patterns were successful in nanografting the Zn (II) porphyrin thiol into ~10-20 nm confined arrangements of circles and frames. The imaging and nanografting imaging forces were ca. 5-8 nN and ca. 20-23 nN, respectively. The physical height of the nanografted Zn (II) porphyrin thiol was determined to be ~3-6 Å above the *n*-dodecanethiol background matrix, which has proved that a monolayer of the molecule has been formed to have a physical height of 15-18 Å. Future steps of this research include method transfer of the AFM gold sample to the STM for future analysis of the charge transport properties of the 10 nm domain size of the Zn (II) porphyrin thiol islands. From this directed assembly technique, physical height and information on the electrochemical properties of the aggregate, such as controllable bias-induced switching of the porphyrin molecules, can

be deciphered by use of Scanning Tunneling Microscopy (STM). This research will aid the development of nanoscaled and molecularly enhanced technology devices.

REFERENCES

(1) Liu, M.; Amro N.A.; Liu, G. *Annual Review of Physical Chemistry* **2008,** *59*, 367.

(2) Love, J. C.; Estroff, L. A.; Kriebel, J. K.; Nuzzo, R. G.; Whitesides, G. M. *Chemistry Review* **2005**, *105*, 1103.

(3) Yamada, H.; Imahori, H.; Nishimura, Y.; Yamazaki, I.; Ahn, T. K.; Kim, S. K.; Kim, D.; Fukuzumi, S. *Journal of the American Chemical Society* **2003**, *125*, 9129.

(4) Joachim, C.; Gimzewski, J. K.; Aviram, A. *Nature* **2000**, *408*, 541.

(5) Tour, J. M.; Jones, L.; Pearson, D. L.; Lamba, J. J. S.; Burgin, T. P.; Whitesides, G. M.; Allara, D. L.; Parikh, A. N.; Atre, S. *Journal of the American Chemical Society* **1995**, *117*, 9529.

(6) Bang, G. S.; Park, J.; Lee, J.; Choi, N.-J.; Baek, H. Y.; Lee, H. *Langmuir* **2007**, *23*, 5195.

(7) Seferos, D. S.; Blum, A. S.; Kushmerick, J. G.; Bazan, G. C. *Journal of the American Chemical Society* **2006**, *128*, 11260.

(8) Watcharinyanon, S.; Nilsson, D.; Moons, E.; Shaporenko, A.; Zharnikov, M.; Albinsson, B.; Martensson, J.; Johansson, L. S. O. *Physical Chemistry Chemical Physics* **2008**, *10*, 5264.

(9) Cao, Z.; Gu, N.; Gong, F.-C. *Materials Science and Engineering: C* **2007**, *27*, 773.

(10) Koehorst, R.; Boschloo, G.K.; Savenije, T.J. *The Journal of Physical Chemistry B* **2000**, *104*, 2371.

(11) Martin, N.; Guldi, D.M. *Chemistry and Engineering News* **2005**, *83*, (8), 32.

(12) Amao, Y.; Asai, K.; Miyakawa, K.; Okura, I. *J. Porphyrins Phthalocyanines* **2000**, *4*, 19-22.

(13) Anariba, F.; Schmidt, L.; Muresan, A. Z.; Lindsey, J.S.; Bocian, D. F., *Langmuir* **2008**, 24, (13), 6698-6704.

(14) Paolesse, R.; Lvova, L.; Nardis, S.; Di Natale, C.; D'Amico, A.; Lo Castro, F. *Microchimica Acta* **2008**, *163*, 103.

(15) Paolesse, R. D. M.; La Monica, L.; Venanzi, M.; Froiio, A.; Nardis, S.; Di Natale, C.; Martinelli, E.; D'Amico, A. *Chemistry - A European Journal* **2002**, *8*, 2476.

(16) Lysenko, A.B.; Thamyongkit, P.; Schmidt, I.; Diers, J.R.; Bocian, D.F.; Lindsey, J.S. *Journal of Porphyrins and Phthalocyanines* **2006**, *10*, (1), 22.

(17) Giribabu, L. K.; Vikay, C. H.; Raghavender, M.; Somaiah, K.; Reddy, P.; Rao, Yella; Venkateswara, P. *Journal of Chemical Sciences* **2008**, *120*, 455.

(18) Chan, Y.H; Schuckman, A.; Perez, L.; Vinodu, M.; Drain, C.; Batteas, J.D. *Journal of Physical Chemistry C* **2008**, *112*, 6110.

(19) Hunter, C. A.; Sanders, J. K. M. *J. Am. Chem. Soc.* **1990**, *112*, (14), 5525.

(20) Anariba, F.; Viswanathan, U.; Bocian, D.F.; McCreery, R.L. *Anal. Chem.* **2006**, *78*, 3104-3112.

(21) Kim, K.-S.; Lin, Z.; Shrotriya, P.; Sundararajan, S.; Zou, Q. *Ultramicroscopy* **2008,** *108* (9), 911-920.

CONTACT INFORMATION

Name:	Kathryn M. Webb
Professional Address:	c/o Dr. James D. Batteas Department of Chemistry Texas A&M University PO BOX 3255 College Station, TX 77843
Email Address:	batteas@mail.chem.tamu.edu kmwebb2010@neo.tamu.edu
Education:	B.S. Chemistry, Minor Business Texas A&M University, May 2010 Undergraduate Research Scholar